Anatomy of nucleon self-energy from equal-time to light-front

Binbin Liu[a], **Chueng-Ryong Ji**[b]

[a] *School of Physics, Beihang University, Beijing, China 100191*,
[b] *Department of Physics, North Carolina State University, Raleigh, North Carolina 27695-8202*

Abstract

Light-front dynamics (LFD) has been of particular interests in hadron physics with the effort of developing the 3D femtography of the nucleon. In this respect, it is important to trace the instantaneous contribution to the fermion propagator in the LFD which involves the constraint degrees of freedom of the fermion. Interpolating the ordinary instant form dynamics (IFD) to the LFD in quantum electrodynamics[15], we have previously identified that the instantaneous contribution to the fermion propagator in the LFD corresponds to the backward moving fermion propagator in the IFD. In this presentation, we discuss this correspondence between the IFD and the LFD in the loop level analyzing the pion loop contribution to the nucleon self-energy in the chiral effective theory. Specifically, we calculate the backward and forward nucleon self-energy interpolating between the IFD and the LFD and trace each part of the contributions to correspond with the light-front instantaneous (LFI) contribution and the on-mass-shell (OMS) contribution in the LFD. The nonanalytic behavior of the pion loop contribution in the nucleon self-energy is anatomically analyzed to confirm the correspondence of each part between the IFD and the LFD unambiguously. Our numerical results exhibiting the entire profile of the interpolating parameter and the momentum (p^z) dependence of the forward and backward moving parts further clarify any conceivable confusion in the prevailing notion of the equivalence between the LFD and the infinite momentum frame ($p^z \to \infty$) approach in the IFD. We also discuss the light-front zero-mode issue contrasting the results in $p^z \to \infty$ and $p^z \to -\infty$.

1 Introduction

In the relativistic particle systems, Dirac proposed the three different forms of the relativistic Hamiltonian dynamics in 1949 [1] i.e., the instant ($x^0 = 0$), front ($x^+ = (x^0 + x^3)/\sqrt{2} = 0$), and point forms. While the instant form dynamics (IFD) of quantum field theories is based on the usual equal time $t = x^0$ quantization, the equal light-front time $\tau \equiv (t + z/c)/\sqrt{2} = x^+$ quantization yields the front form dynamics, more commonly called light-front dynamics (LFD), correspondingly. The point form dynamics has also been studied [2], but it is not our concern in this work.

Nucleon-pion loop is fundamental in particle physics. According to approximate chiral symmetry of QCD, the pion cloud of the nucleon plays a vital role in understanding the

nucleon's long-range structure by making vital corrections to static nucleon properties, such as the mass, magnetic moment and axial charge. The pion cloud also affects electric and magnetic charge distributions of nucleons[8]. Having a pseudoscalar property, the pion emission from a nucleon gives a nontrivial redistribution of the spin and angular momentum of its quark constituents[9], partially resolving the proton spin problem[10]. In this work, we take the nucleon-pion loop as an example to illustrate the LFI contribution by splitting the nucleon-pion loop into forward and backward in the LFD.

The interpolating dynamics traces a dramatic change of the the longitudinal boost characteristics between the two different forms of dynamics, namely, from 'dynamic' in IFD to 'kinematic' in LFD. Following the convention of space-time coordinates, the interpolating angle in the interpolating dynamics can be defined [3], [11]-[13] as:

$$\begin{bmatrix} x_{\hat{+}} \\ x_{\hat{-}} \end{bmatrix} = \begin{bmatrix} \cos[\delta] & \sin[\delta] \\ \sin[\delta] & -\cos[\delta] \end{bmatrix} \begin{bmatrix} x^0 \\ x^3 \end{bmatrix} \tag{1}$$

in which the interpolation angle is allowed to change smoothly from 0 through 45 degree, $0 \leq \delta \leq \pi/4$. All the indices with the widehat notation signify the variables with the interpolation angle δ. For the limit $\delta \to 0$ we have $x_{\hat{+}} = x_0$ and $x_{\hat{-}} = -x_3$ so that we recover usual space-time coordinates although the z-axis is inverted. For the other extreme limit, $\delta \to \pi/4$, we have $x_{\pm} = (x_0 \pm x_3)/\sqrt{2}$ which leads to the standard light-front coordinates. In interpolating dynamics, all 4-vectors, such as 4-momentums, should be written in terms of interpolation angle by Eq.(1).

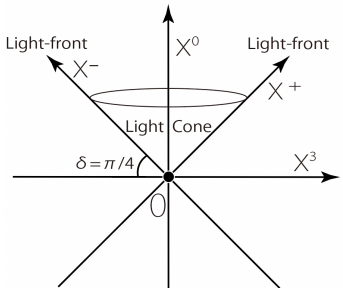

Figure 1: The LFD in relation with the IFD by an ID parameter $\delta = \pi/4$.

The interpolating form plays important role in relating the LFD calculations with those in the IFD. In LFD, special care is needed for consideration of the zero modes which are spurs of end-point singularities. A smoothly changing interpolation angle may help one safely move from instant to light-front form without naively ignoring those singularities. Hence establishing physics theories in the interpolating dynamics is meaningful by giving us a chance to trace from the IFD to the LFD.

Previously, interpolating dynamics has been applied in some theories. In Ref. [13], the authors have developed the electromagnetic gauge field propagator interpolated between the IFD and the LFD. In Ref. [14], the authors have derived the generalized helicity spinor connecting the instant form helicity spinor to the light-front helicity spinor, followed by Ref. [15], in which Ji et. al have constructed the interpolating quantum electrodynamics theory. However, interpolation to our knowledge has not been made in computing the pion loop, such as the nucleon self-energy.

In this paper, we identify the LNA of the LFI loop contribution from the backward nucleon self-energy and the corresponding forward contribution in the LFD. Then with interpolating parametrization, we trace the LNA behaviors for each parts from the LFD to IFD along

special lines, which we assume as "frames" X and Y, and identify the emergent LF zero model contribution. With numerical technics, we trace on the entire form-frame profile the each contributions of the nucleon self-energy (in three different manners), which give figurative illustrations about how each part of the nucleon self-energy evolves with respect of forms and frames. When it comes to the IMF and the LFD, there appears conceivable confusions in the equivalence between them. Our results in this work clarify such confusions with the interpretation dynamics.

2 Definitions

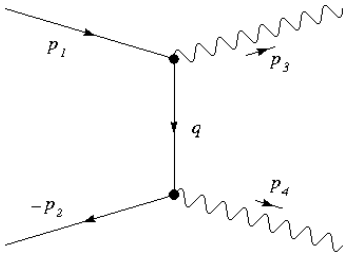

Figure 2: Feynman diagram for $e^+e^- \to \gamma\gamma$ process. While this figure is drawn for the t-channel Feynman diagram, the crossed channel (or u-channel) can be drawn by crossing the two final state particles.

We begin by presenting the definitions for the nucleon self-energy and its decompositions in the tree level. The intermediate virtual fermion propagator in Fig. 2 is

$$\Sigma_N = \frac{\not{q} + M}{q^2 - M^2} \tag{2}$$

Following [15], in interpolating dynamics the nucleon/fermion propagator Σ_N (and hence the nucleon self-energy which we will talk later) can be decomposed in two parts, i.e. forward and backward moving part

$$\Sigma_N = \Sigma_{Na} + \Sigma_{Nb} = \frac{\not{Q}_a \ + M}{2Q^{\widehat{+}}(q_{\widehat{+}} - Q_{a\widehat{+}})} + \frac{-\not{Q}_b \ + M}{2Q^{\widehat{+}}(-q_{\widehat{+}} - Q_{b\widehat{+}})} \tag{3}$$

as shown in Figs. 3a and 3b. M is the nucleon mass and

$$Q_a = \left(\frac{-\mathbb{S} q_{\widehat{-}} + Q^{\widehat{+}}}{\mathbb{C}},\ q_\perp,\ q_{\widehat{-}} \right)$$

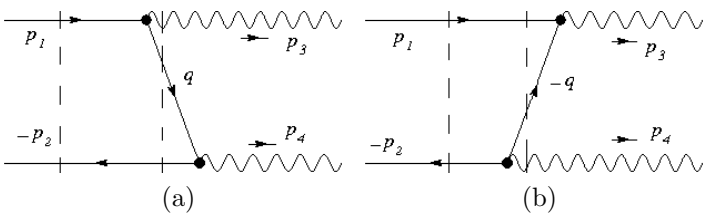

Figure 3: Time-ordered diagrams (a) and (b) for $e^+e^- \to \gamma\gamma$ annihilation process. The u-channel amplitudes can be obtained by crossing the two final state particles.

$$Q_b = \left(\frac{\mathbb{S} q_{\widehat{-}} + Q^{\widehat{+}}}{\mathbb{C}}, \ -q_\perp, \ -q_{\widehat{-}} \right)$$
$$Q^{\widehat{+}} = \sqrt{q_{\widehat{-}}^2 + \mathbb{C}(q_\perp^2 + M^2)}, \tag{4}$$

and the four-momentum of external nucleon is denoted by q. Here we capitalize the q to Q which means there have been applied the on-mass shell condition $q^2 = M^2$. Eq.(3) is the on-mass-shell version of the nucleon forward and backward moving parts in tree level.

We also introduce Σ'_{Nb} and Σ'_{Na} as the off-shell-version of Σ_{Nb} and Σ_{Na}. Practically, we do it by changing the Q_b and Q_a into $-q$ and q where $q = \left(q_{\widehat{+}}, \ q_\perp, \ q_{\widehat{-}}\right)$, and the four-momentum square q^2 and can be expanded in interpolating dynamics (ID) as

$$q^2 = \mathbb{C}(q_{\widehat{+}}^2 - q_{\widehat{-}}^2) + 2\mathbb{S} q_{\widehat{+}} q_{\widehat{-}} - q_\perp^2, \tag{5}$$

denoting $\mathbb{S} = \sin(2\delta)$, $\mathbb{C} = \cos(2\delta)$. The off-mass-shell contribution of backward and forward moving decompositions read

$$\Sigma'_{Nb} = \frac{\not{q} + M}{2Q^{\widehat{+}}(-q_{\widehat{+}} - Q_{b\widehat{+}})} = \frac{\mathbb{C}(\not{q} + M)}{2Q^{\widehat{+}}(\mathbb{C} q_{\widehat{+}} + \mathbb{S} q_{\widehat{-}} + Q^{\widehat{+}})} \tag{6}$$

and

$$\Sigma'_{Na} = \frac{\not{q} + M}{2Q^{\widehat{+}}(q_{\widehat{+}} - Q_{a\widehat{+}})}. \tag{7}$$

When taking the LF limit ($\mathbb{C} \to 0$ and $\mathbb{S} \to 1$), the backward moving off-mass shell part approaches to 0, as $\Sigma'_{Nb} \to \frac{\mathbb{C}(\not{q}+M)}{2q^+(q^+ + q^+)} \to 0$, where $q_{\widehat{-}} \to q^+$ has been used. Correspondingly, the $\Sigma'_{Na} \to \Sigma_N$. The following is the proof. In LF, we can expand $Q^{\widehat{+}}$ as

$$Q^{\widehat{+}} \approx q_{\widehat{-}} \left(1 + \frac{\mathbb{C}(q_\perp^2 + M^2)}{2q_{\widehat{-}}^2} \right), \tag{8}$$

and hence in LFD

$$Q_{a\widehat{+}} \to \frac{M^2 + q_\perp^2}{2q^+}. \tag{9}$$

The denominator in LFD then becomes

$$2Q^{\widehat{+}} \left(q_{\widehat{+}} - Q_{a\widehat{+}} \right) \to 2q^+ \left(q^- - \frac{M^2 + q_\perp^2}{2q^+} \right) = q^2 - M^2 \tag{10}$$

So we have

$$\Sigma'^{LFD}_{Na} \to \frac{\not{q} + M}{q^2 - M^2} = \Sigma_N. \tag{11}$$

To assist later calculations, we may define a "remnant part" Σ_{NRP}, which is subtraction of the Σ_{Nb} from Σ'_{Nb}, where the "N" in the subscript means that the definition is related with the nucleon propagator in tree level

$$\Sigma_{NRP} = \Sigma_{Nb} - \Sigma'_{Nb} = \frac{\gamma^{\widehat{+}}}{2Q^{\widehat{+}}}. \tag{12}$$

correspondingly,

$$\Sigma_{NRP} = -\Sigma_{Na} + \Sigma'_{Na}, \tag{13}$$

as

$$\Sigma'_{Na} + \Sigma'_{Nb} = \Sigma_{Na} + \Sigma_{Nb} = \Sigma_N. \tag{14}$$

The Σ_{Nb} and Σ_{Na} in the LFD becomes,

$$\Sigma_{Nb}^{LFD} = \Sigma_{NRP}^{LFD} = \Sigma_{NLFI} = \frac{\gamma^+}{2q^+} \tag{15}$$

where the Σ_{NRP}^{LFD} is getting from pushing the Σ_{NRP} into the LFD, and is actually the so-called LF instantaneous (LFI) contribution Σ_{NLFI} in the tree level. Correspondingly,

$$\Sigma_{Na}^{LFD} = \Sigma_{NOMS} = \Sigma_N - \Sigma_{NLFI}, \tag{16}$$

where the Σ_{NOMS} is the tree level expression of the on-mass-shell contribution, which can be obtained from subtracting the tree level LFI contribution Σ_{NLFI} from the nucleon propagator Σ_N.

Above, we define the forward and backward moving parts of the nucleon propagator in the tree level. In the following, we define their correspondence in loop level.

We begin with the nucleon self-energy shown in Fig. 4 where intermediate momentum $p_N = p - k$ is substituted in all the qs in the tree level formulations. Using relative Feynman

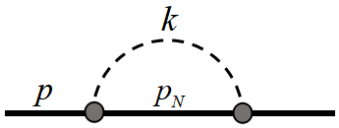

Figure 4: Feynman diagram of nucleon pion loop with $p_N = p - k$

rules [17] and interpolating gamma matrixes and spinors[15], we can write down the self-energy operator of the nucleon dressing with a pion propagator,

$$\begin{aligned}\hat{\Sigma} =& i\left(\frac{g_A}{2f_\pi}\right)^2 \int \frac{d^4k}{(2\pi)^4}(\not{k}\gamma^5\vec{\tau})\frac{i(\not{p}_N + M)}{p_N^2 - M^2 + i\epsilon}(\gamma^5\not{k}\vec{\tau}) \\ & \times \frac{i}{k^2 - m_\pi^2 + i\epsilon}.\end{aligned} \tag{17}$$

where M is the nucleon mass, m_π is the pion mass, and p in p_N is the external momentum satisfying $p^2 = M^2$ where M is the external nucleon mass. Besides, $g_A = 1.267$ is the axial vector charge of the nucleon, and $f_\pi \approx 0.093GeV$ is the pion decay constant. $\vec{\tau}$ is the Pauli matrix operator, whose square is 3. Note that here we use the interpolating dynamics, so the $\not{p}_N = p_{\hat{\mu}}\gamma^{\hat{\mu}}$ with $\not{p} = p_{\hat{\mu}}\gamma^{\hat{\mu}}$ and $\not{k} = k_{\hat{\mu}}\gamma^{\hat{\mu}}$ which have the hat notations. For convenience, we make contracted definitions for the denominators of the nucleon and pion propagators, as follows

$$D_N = p_N^2 - M^2 + i\epsilon \tag{18}$$

$$D_\pi = k^2 - m_\pi^2 + i\epsilon. \tag{19}$$

Since $\{\gamma^5, \gamma^\mu\} = 0$ and $(\gamma^5)^2 = I$, we have

$$\hat{\Sigma} = -3\left(\frac{g_A}{2f_\pi}\right)^2 \int \frac{d^4k}{(2\pi)^4} \not{k} \frac{-\not{p}_N + M}{D_N} \not{k} \frac{i}{D_\pi}. \tag{20}$$

Performing the spin sum calculation, we get

$$\Sigma = \frac{1}{2}\sum_s \bar{u}(p,s)\hat{\Sigma}u(p,s) = \frac{1}{2}\mathrm{Tr}\left[\frac{\not{p}+M}{2M}\hat{\Sigma}\right]. \tag{21}$$

After solving the trace, we get,

$$\Sigma = -i3\left(\frac{g_A}{2f_\pi}\right)^2 \int \frac{d^4k}{(2\pi)^4} \frac{-\left[2(p\cdot k)(k\cdot p_N) - (p\cdot p_N)k^2\right] + M^2k^2}{D_N D_\pi M}. \tag{22}$$

which can be simplified as

$$\Sigma = -i3\left(\frac{g_A}{2f_\pi}\right)^2 \int \frac{d^4k}{(2\pi)^4} \left[\frac{2Mk^2}{D_N D_\pi} + \frac{p\cdot k}{D_\pi M}\right]. \tag{23}$$

To decompose the interpolating nucleon self-energy, we use Eq.(3) in the tree level to the corresponding loop level contributions. Substituting the nucleon propagator in the nucleon self-energy operator Eq.(17) with the Σ_{Ni} (i=a,b) we can get the forward and backward moving part of the nucleon poin loop. For the forward moving part, we have

$$\begin{aligned}\hat{\Sigma}_a =& i\left(\frac{g_A}{2f_\pi}\right)^2 \int \frac{d^4k}{(2\pi)^4} (\not{k}\gamma^5\vec{\tau}) \frac{i(\not{P}_{Na}+M)}{2P_N^{\widehat{+}}(p_{N\widehat{+}} - P_{a\widehat{+}})} (\gamma^5\not{k}\vec{\tau}) \\ & \times \frac{i}{k^2 - m_\pi^2 + i\epsilon}.\end{aligned} \tag{24}$$

where the P_{Na}, and the following P_{Nb} and $P_N^{\widehat{+}}$ are defined by substituting all the qs in Eq.(4) with p_N. Following the procedure of spin sum and trace calculation, we can easily get

$$\Sigma_a = -i3\left(\frac{g_A}{2f_\pi}\right)^2 \int \frac{d^4k}{(2\pi)^4} \frac{\left[-2(p\cdot k)(k\cdot P_{Na}) + (p\cdot P_{Na})k^2\right] + M^2k^2}{2P_N^{\widehat{+}}(p_{N\widehat{+}} - P_{Na\widehat{+}})D_\pi M} \tag{25}$$

For the Σ_b, we can get,

$$\Sigma_b = -i3\left(\frac{g_A}{2f_\pi}\right)^2 \int \frac{d^4k}{(2\pi)^4} \frac{\left[2(p\cdot k)(k\cdot P_{Nb}) - (p\cdot P_{Nb})k^2\right] + M^2k^2}{2P_N^{\widehat{+}}(-p_{N\widehat{+}} - P_{Nb\widehat{+}})D_\pi M} \tag{26}$$

The Feynman diagram for the Σ_a and Σ_b are depicted in Fig. 5a and 5b.

To assist the later calculation, we find the remnant part (Σ_{RP}) in loop level, which is the difference between on-mass-shell and off-mass-shell contributions as we will show later. From

$$\begin{aligned}\hat{\Sigma}_{RP} =& i\left(\frac{g_A}{2f_\pi}\right)^2 \int \frac{d^4k}{(2\pi)^4} (\not{k}\gamma^5\vec{\tau}) \frac{i\gamma^{\widehat{+}}}{2P_N^{\widehat{+}}} (\gamma^5\not{k}\vec{\tau}) \\ & \times \frac{i}{k^2 - m_\pi^2 + i\epsilon}.\end{aligned} \tag{27}$$

we get,

$$\Sigma_{RP} = -i3\left(\frac{g_A}{2f_\pi}\right)^2 \int \frac{d^2k_\perp dk_{\widehat{-}} dk_{\widehat{+}}}{(2\pi)^4} \frac{-[2(p\cdot k)k^{\widehat{+}} - p^{\widehat{+}}k^2]}{2P_N^{\widehat{+}}D_\pi M}. \tag{28}$$

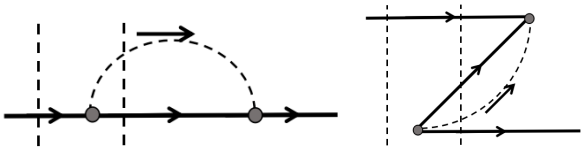

(a) (b)

Figure 5: Time-ordered diagrams (a) and (b) for the forward moving nucleon self-energy (positive energy diagram) and the backward moving nucleon self-energy ("Z" graph).

3 Anatomy of nucleon self-energy into backward and forward moving part in LFD

The backward moving Σ_b shown in Eq.(26), in the LF limit, where $\mathbb{C} \to 0$, becomes

$$\Sigma_b^{LFD} = \Sigma_{LFI} = -\,i3\left(\frac{g_A}{2f_\pi}\right)^2 \int \frac{d^4k}{(2\pi)^4} \frac{-2(p\cdot k)k^+ + k^2 p^+}{2p_N^+ D_\pi M} \tag{29}$$

which is the same with Σ_{RP}^{LFD}, which can also be obtained by pushing Eq.(28) into LFD (note that $P_N^+ = p_N^+$). Therefore the Σ_b^{LFD} is the LFI contribution (Σ_{LFI}) of the nucleon self-energy in the loop level.

Now consider the forward moving part of the nucleon self-energy, Eq.(25) in LFD. When approaching to LF, following Eq.(10), the denominator becomes $2P_N^{\widehat{+}}(p_{N\widehat{+}} - P_{Na\widehat{+}})D_\pi M \to D_N D_\pi M$. The P_{Na}, in the LF limit, becomes $P_{Na}^{LFD} = \left(\frac{(p_\perp - k_\perp)^2 + M^2}{2(p^+ - k^+)}, p_\perp - k_\perp, p^+ - k^+\right)$. Therefore, the interpolating forward moving part of the nucleon self-energy becomes, in LF limit,

$$\Sigma_a^{LFD} = -\,i3\left(\frac{g_A}{2f_\pi}\right)^2 \int \frac{d^4k}{(2\pi)^4} \frac{-\left[2(p\cdot k)(k\cdot P_{Na}^{LFD}) - (p\cdot P_{Na}^{LFD})k^2\right] + M^2k^2}{D_N D_\pi M}. \tag{30}$$

In the following, we perform the detailed calculation for the Σ_{LFI} and Σ_a^{LFD}.

3.1 Identify the LF instantaneous contribution

Starting from Eq.(29), with some transformations, we have

$$\Sigma_{LFI} = -\,i3\left(\frac{g_A}{2f_\pi}\right)^2 \int \frac{d^2k_\perp dk^- dk^+}{(2\pi)^4} \left\{\frac{p\cdot k}{D_\pi M} + \frac{p^+[k^2 - 2(p\cdot k)]}{2(p^+ - k^+)MD_\pi}\right\}. \tag{31}$$

where the first term is zero, because of oddity in k. The second term, i.e. the LFI contribution, after some simplifications becomes

$$\Sigma_{LFI} = -\,i3\left(\frac{g_A}{2f_\pi}\right)^2 \int \frac{d^2k_\perp dk^- dk^+}{(2\pi)^4} \frac{p^+}{2M}\left[\frac{1}{(p^+ - k^+)} + \frac{m_\pi^2}{(p^+ - k^+)D_\pi} - \frac{2p\cdot k}{(p^+ - k^+)D_\pi}\right] \tag{32}$$

In order to explicitly calculate the LFI part, we need to regulate the divergence of the integrand. Here we choose the Pauli-Villars (PV) regularization. The reason for using the Pauli-Villars regularization is that it is a covariant regularization, with which we are able to

regularize in a covariant manner, which allows us to show the exact equivalence of the entire nucleon self-energy invariant under the Lorentz transformation regardless of the form taken in the computation, e.g. whether it's LFD or the IFD in IMF or rest frame, etc. Besides, Ji et al. [19] have shown that the Pauli-Villars regularization in the example of quantum electrodynamics is naturally realized in the Bopp-Podolsky's generalized electrodynamics [20]. The Pauli-Villars mass parameter Λ here corresponds to the inverse of the length dimensional parameter associated with Bopp-Podolsky's higher order derivatives [20].

The PV regularization is by substituting $\frac{1}{D_\pi}$ in the denominators with

$$\frac{-\Lambda^2}{D_\pi D_\Lambda} = \frac{-\Lambda^2}{D_\Lambda - D_\pi}\left(\frac{1}{D_\pi} - \frac{1}{D_\Lambda}\right) = \frac{-\Lambda^2}{m_\pi^2 - \Lambda^2}\left(\frac{1}{D_\pi} - \frac{1}{D_\Lambda}\right). \tag{33}$$

where the $D_\Lambda = k^2 - \Lambda^2 + i\epsilon$ and when $\Lambda >> m_\pi$ the $\frac{-\Lambda^2}{D_\pi D_\Lambda}$ goes back to $1/D_\pi$. The $i\epsilon$ is add for the same purpose which is to shift the pole out of the real axis. Equivalently, one can multiply the form factor $\frac{-\Lambda^2}{D_\Lambda}$ which approaching to 1 when $\Lambda \to \infty$, with the divergent integrand. Note that we add nF in the subscript to discriminate how much time the PV form factor has been applied. For example, we get

$$\begin{aligned}\Sigma_{LFI:1F} =& \frac{-\Lambda^2}{D_\Lambda}\Sigma_{LFI} \\ =& -i3(-\Lambda^2)\left(\frac{g_A}{2f_\pi}\right)^2 \int \frac{d^2k_\perp dk^- dxp^+}{(2\pi)^4}\frac{1}{2M}\left[\frac{1}{(1-x)D_\Lambda} + \frac{m_\pi^2}{(1-x)D_\pi D_\Lambda} - \frac{2p^+k^- + 2p^-p^+x}{(1-x)D_\pi D_\Lambda}\right]\end{aligned} \tag{34}$$

where the 1F in the denominator means the Pauli-Villar form factor $\frac{-\Lambda^2}{D_\Lambda}$ has been multiplied for one time (later we will have higher times), and we use the momentum fraction defined as $x = k^+/p^+$, also we choose the $p_\perp = 0$ here and in the following of the paper for simplification. According to [18], in the point-like theory, we have

$$\int dk^- \frac{1}{D_\pi} = \pi i \log\left[\frac{k_\perp^2 + m_\pi^2}{\mu^2}\right]\frac{\delta[x]}{p^+} \tag{35}$$

where the μ is the regularization mass parameter. Therefore, the first term becomes

$$\int dxp^+ \int dk^- \frac{1}{(1-x)D_\Lambda} = \pi i \int dx \log\left[\frac{k_\perp^2 + \Lambda^2}{\mu^2}\right]\frac{\delta[x]}{(1-x)} = \pi i \log\left[\frac{k_\perp^2 + \Lambda^2}{\mu^2}\right] \tag{36}$$

where all the p^+s are canceled and only the $x = 0$ contribute to the integration. Since the integration range is limited to $0 < x < 1$ in the LFD, we have includes the LF zero mode contribution where $p^+ = 0$ or $p^z \to -\infty$. For the second term, doing the subtraction following the procedure of the Pauli-Villars regularization, we get

$$\int dxp^+ \int dk^- \frac{m_\pi^2}{(1-x)D_\pi D_\Lambda} = \int dxp^+ \int dk^- \left(\frac{1}{D_\pi} - \frac{1}{D_\Lambda}\right)\frac{m_\pi^2}{(1-x)(m_\pi^2 - \Lambda^2)} \tag{37}$$

$$= \int dx \frac{\pi i m_\pi^2}{(1-x)(m_\pi^2 - \Lambda^2)} \log\left[\frac{k_\perp^2 + m_\pi^2}{k_\perp^2 + \Lambda^2}\right]\delta[x] = \frac{\pi i m_\pi^2}{m_\pi^2 - \Lambda^2}\log\left[\frac{k_\perp^2 + m_\pi^2}{k_\perp^2 + \Lambda^2}\right]. \tag{38}$$

which is again independent of the p^+. The $2p^-p^+x$ term in the third term contributes zero due to the $\delta[x]$,

$$\int dxp^+ \int dk^- \frac{2p^-p^+x}{(1-x)D_\pi D_\Lambda} \sim \int dx \frac{x\delta[x]}{1-x} = 0. \tag{39}$$

Performing the derivatives to the $\frac{1}{D_\pi}$ with respect of k^+ (or x) (note that in LFD, $k^2 = 2k^+k^- - k_\perp^2$), then doing indefinite integration with respect of m_π^2, and multiplying with $-p^+$, where the minus sign is to reverse the sign change caused by doing the derivatives of k^+, we get

$$\begin{aligned}
&\int dk^- \frac{2p^+k^-}{D_\pi} = -p^+ \int d(m_\pi^2) \frac{\partial}{\partial x} \int dk^- \frac{1}{D_\pi} \\
&= -\int d(m_\pi^2) \pi i \log\left[\frac{k_\perp^2 + m_\pi^2}{\mu^2}\right] \frac{d}{dx}\frac{\delta[x]}{p^+} = -\pi i \left[-m_\pi^2 + (k_\perp^2 + m_\pi^2)\log\left[\frac{k_\perp^2 + m_\pi^2}{\mu^2}\right]\frac{d}{dx}\frac{\delta[x]}{p^+}\right]
\end{aligned} \tag{40}$$

Note that after the indefinite integration of m_π^2, there comes a constant term that is independent of m_π^2, and we set it to be zero here for convenience. If it is non-zero, it would be canceled out in the later PV regularization.

To get the result with D_Λ in the denominator, one can simply change the m_π in the equation above into Λ. Following the Eq.(37) to do the subtraction, the third term can be calculated as

$$\begin{aligned}
&\int dx p^+ \int dk^- - \frac{2p^+k^- + 2p^-p^+x}{(1-x)D_\pi D_\Lambda} = \int dx p^+ \int dk^- \frac{-2p^+k^-}{(1-x)D_\pi D_\Lambda} \\
&= \int dx \frac{i\pi}{m_\pi^2 - \Lambda^2} \frac{d(\delta[x])}{dx} \frac{1}{1-x} \\
&\left[\left(\Lambda^2 + k_\perp^2\right)\log\left[\frac{k_\perp^2 + \Lambda^2}{k_\perp^2 + m_\pi^2}\right] - \left(m_\pi^2 - \Lambda^2\right)\log\left[k_\perp^2 + m_\pi^2\right] + \left(m_\pi^2 - \Lambda^2\right)\log[\mu^2]\right] \\
&= \frac{i\pi}{m_\pi^2 - \Lambda^2}\left[\left(\Lambda^2 + k_\perp^2\right)\log\left[\frac{k_\perp^2 + \Lambda^2}{k_\perp^2 + m_\pi^2}\right] - \left(m_\pi^2 - \Lambda^2\right)\log\left[k_\perp^2 + m_\pi^2\right] + \left(m_\pi^2 - \Lambda^2\right)\log[\mu^2]\right].
\end{aligned} \tag{41}$$

All the momentum dependence is canceled explicitly during the calculation, in agreement with the frame invariance of LFD.

The three terms added together are still divergent in the $k_\perp$ integration. One can basically do the Pauli-Villars regularization for sufficient amount of time to the integrand of the divergent integration to make it convergent, and here we introduce another method to easily raise the power of the Pauli-Villars regulator $1/D_\Lambda$ to achieve the required convergence. First, we introduce the notation Σ_x as the subject to be applied the derivative technique, and the technique is then explained as follows

$$\Sigma_{x:nF} = \frac{(-\Lambda^2)^n (m-1)!}{(n-1)!} \frac{\partial^{n-1}}{\partial(\Lambda^2)^{n-1}} \frac{\Sigma_{x:mF}}{(-\Lambda^2)^m} \tag{42}$$

with $n > m$, where the nF and mF in the subscript represent the number of PV form factor multiplied to the subject Σ_x, and the Σ_x either means the integrand of Σ_x if the integration is not finished or means the final results of Σ_x after integration, x represents the label for the physical quantities, and in this section stands for LFI. Here, we have m=1 and we choose n=4 for the integrations. After raising the power for the form factor using Eq.(42), we perform the transverse integration, and get

$$\Sigma_{LFI:4F} = -\frac{g_A^2 \Lambda^8}{256 M f_\pi^2 \pi^2}\left(-\frac{\Lambda^4 + \frac{2m_\pi^6}{\Lambda^2} - 6\Lambda^2 m_\pi^2 + 6m_\pi^4 \log\left[\frac{\Lambda^2}{m_\pi^2}\right] + 3m_\pi^4}{2\left(\Lambda^2 - m_\pi^2\right)^4}\right) \tag{43}$$

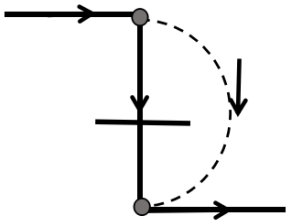

Figure 6: Time-ordered diagram for the LF instantaneous contribution Σ_{LFI}.

The corresponding leading non-analytic behavior is

$$\Sigma_{LFI}^{LNA} = -\frac{3g_A^2}{32\pi f_\pi^2}\left(\frac{m_\pi^4 \log[m_\pi^2]}{8M\pi} + \mathcal{O}(m_\pi^5)\right). \tag{44}$$

The above calculations indicate that the LF instantaneous contribution is coming from the internal pion zero mode, i.e. $x = 0$, with $k^+ = 0$, instead of the external nucleon zero mode $p^+ = 0$. The $\pi^\pm$ are created from the vacuum fluctuation and then annihilating back to the vacuum, during which the π^+ touch the nucleon instantaneously. The diagram of the LF instantaneous contribution is depicted in Fig. 6.

3.2 Calculate the forward moving part in LFD

To calculate the forward moving contribution of the nucleon self-energy in LFD, we substitute all the p in the Eq.(30) with $p_N + k$, which after some simplifications yields

$$\Sigma_a^{LFD} = -i3\left(\frac{g_A}{2f_\pi}\right)^2 \int \frac{d^4k}{(2\pi)^4} \frac{(P_{Na}^{LFD}\cdot k)}{D_\pi M} + \frac{(M^2 + p_N \cdot P_{Na}^{LFD})k^2}{D_N D_\pi M} \tag{45}$$

The first term in the above equation, after expanding the inner product, becomes

$$\frac{P_{Na}^{LFD}\cdot k}{D_\pi M} = \frac{\frac{[(p_\perp - k_\perp)^2 + M^2]k^+}{2(p^+ - k^+)} + k^-(p^+ - k^+) - k_\perp(p_\perp - k_\perp)}{D_\pi M} \tag{46}$$

$$\tag{47}$$

which after putting into the on mass shell condition $M^2 = 2p^+p^- - p_\perp^2$, can be simplified as

$$\frac{P_{Na}^{LFD}\cdot k}{D_\pi M} = -\frac{p^+k^2 - 2k^+(p\cdot k)}{2(p^+ - k^+)D_\pi M} + \frac{p\cdot k}{D_\pi M} - \frac{k^2}{2D_\pi M}. \tag{48}$$

where the first term corresponds to the $-\Sigma_{LFI}$, as suggested by Eq.(29). For the second term in Eq.(45), also expanding the inner product, we get

$$\frac{(M^2 + p_N \cdot P_{Na}^{LFD})k^2}{D_N D_\pi M} = \frac{2M^2k^2}{D_N D_\pi M} + \frac{k^2}{2D_\pi M} \tag{49}$$

Therefore adding the two terms together, the Σ_a^{LFD} becomes

$$\Sigma_a^{LFD} = -i3\left(\frac{g_A}{2f_\pi}\right)^2 \int \frac{d^4k}{(2\pi)^4}\left[\frac{p\cdot k}{D_\pi M} + \frac{2Mk^2}{D_N D_\pi}\right] - \Sigma_{LFI} \tag{50}$$

where the terms in the square bracket is the entire nucleon self-energy in loop level, i.e. Σ in Eq.(23), meaning that

$$\Sigma_a^{LFD} = \Sigma - \Sigma_{LFI}. \tag{51}$$

LNA $\left(/\frac{-3g_A^2}{32\pi f_\pi^2}\right)$	LFD(p^z independent)
Σ_a^{LFD}	$m_\pi^3+\frac{3}{8\pi}\frac{m_\pi^4\log[m_\pi^2]}{M}$
$\Sigma_b^{LFD}=\Sigma_{LFI}$	$\frac{1}{8\pi}\frac{m_\pi^4\log[m_\pi^2]}{M}$
Σ	$m_\pi^3+\frac{1}{2\pi}\frac{m_\pi^4\log[m_\pi^2]}{M}$

Table 1: The LNA of the forward and backward parts of, and the entire nucleon self-energy in the LFD which is frame invariant.

In order to get the Σ_a^{LFD}, we only need to obtain the Σ. Since the integration for Σ is also divergent originally, one can regularize it by applying the Pauli-Villars regularization. To be consistent, we also multiply the PV form factor $\frac{\Lambda^4}{D_\Lambda^2}$ with Σ in Eq.(23) to get Σ_{4F}. Therefore, we have

$$\begin{aligned}
\Sigma_a^{LFD:4F} =& \frac{\Lambda^4 g_A^2}{64M\pi^2\left(4M^2-\Lambda^2\right)^3 f_\pi^2\left(\Lambda^2-m_\pi^2\right)^4}\left\{\Lambda^2\left(-4M^2+\Lambda^2\right)*\left(-2M^4\Lambda^6+2M^2\Lambda^8-6M^4\Lambda^4m_\pi^2\right.\right.\\
&-3M^2\Lambda^6m_\pi^2+18M^4\Lambda^2m_\pi^4-10M^4m_\pi^6+M^2\Lambda^2m_\pi^6-3\left(-4M^2\Lambda+\Lambda^3\right)^2\log\left[\frac{\Lambda^2}{m_\pi^2}\right]m_\pi^4\\
&-6\left(-4M^2\Lambda+\Lambda^3\right)^2\left(\arctan\left[\frac{m_\pi}{\sqrt{2M-m_\pi}\sqrt{2M+m_\pi}}\right]+\arctan\left[\frac{2M^2-m_\pi^2}{\sqrt{2M-m_\pi}m_\pi\sqrt{2M+m_\pi}}\right]\right)\\
&\times\sqrt{2M-m_\pi}\left(-m_\pi\right)^{5/2}\sqrt{-m_\pi\left(2M+m_\pi\right)}\Big)+6\sqrt{4M^2\Lambda^2-\Lambda^4}\left(36M^6\Lambda^2m_\pi^4-4M^6m_\pi^6\right.\\
&\left.+\Lambda^8\left(2M^4+2M^2m_\pi^2-m_\pi^4\right)-2\Lambda^6\left(2M^6+10M^4m_\pi^2-5M^2m_\pi^4\right)+6\Lambda^4\left(6M^6m_\pi^2-5M^4m_\pi^4\right)\right)\\
&\left.\left(\arctan\left[\frac{\Lambda}{\sqrt{4M^2-\Lambda^2}}\right]-\arctan\left[\frac{-2M^2+\Lambda^2}{\sqrt{4M^2\Lambda^2-\Lambda^4}}\right]\right)\right\}\\
&-\frac{g_A^2\Lambda^8}{256Mf_\pi^2\pi^2}\left(-\frac{\Lambda^4+\frac{2m_\pi^6}{\Lambda^2}-6\Lambda^2m_\pi^2+6m_\pi^4\log\left[\frac{\Lambda^2}{m_\pi^2}\right]+3m_\pi^4}{2\left(\Lambda^2-m_\pi^2\right)^4}\right)
\end{aligned}\tag{52}$$

with LNA behaviors,

$$\Sigma_a^{LFD:LNA}=-\frac{3g_A^2}{32\pi f_\pi^2}\left(m_\pi^3+\frac{3m_\pi^4\log[m_\pi^2]}{8M\pi}+\mathcal{O}(m_\pi^5)\right).\tag{53}$$

The LNA for both Σ_{LFI} and Σ_a^{LFD} are summarized in Tab. 1.

4 Trace the backward and forward moving part in LNA

We now use interpolating parameters to trace the LFD results, and see their LNA behavior in other dynamical forms with specific frames.

For convenience, we decompose the Σ_a and Σ_b and find their off-mass-shell versions $\Sigma_a^{'}$ and $\Sigma_b^{'}$ by adding and subtracting the Σ_{RP}, i.e,

$$\Sigma_a=\Sigma_a^{'}-\Sigma_{RP}$$

$$\Sigma_b = \Sigma_b^{'} + \Sigma_{RP} \tag{54}$$

To get the LNA, we can work on the two parts respectively. We take the Σ_a as an example for illustration. In the interpolating dynamics, substituting the P_{Nb} and expanding the four-momentum, after some simplifications, we have

$$\begin{aligned}\Sigma_a = & -i3\left(\frac{g_A}{2f_\pi}\right)^2 \int \frac{d^4k}{(2\pi)^4 2P_N^{\widehat{+}}(p_N^{\widehat{+}} - P_N^{\widehat{+}})D_\pi M}\left[-2(p\cdot k)\left(-k_{\widehat{-}}p_{N\widehat{-}} + P_N^{\widehat{+}}k^{\widehat{+}} - \mathbb{C}k_\perp p_{N\perp}\right)\right. \\ & \left. + k^2\left(-p_{\widehat{-}}p_{N\widehat{-}} + P_N^{\widehat{+}}p^{\widehat{+}} - \mathbb{C}p_\perp p_{N\perp}\right) + \mathbb{C}M^2k^2\right].\end{aligned} \tag{55}$$

Adding the Σ_{RP} in Eq.(28) to Σ_a, we can get the $\Sigma_a^{'}$,

$$\Sigma_a^{'} = -i3\left(\frac{g_A}{2f_\pi}\right)^2 \int \frac{d^4k}{(2\pi)^4}\frac{-2(p\cdot k)^2 + k^2(p\cdot k) + 2k^2M^2}{2P_N^{\widehat{+}}M(p_{N\widehat{+}} - P_{Na\widehat{+}})D_\pi}. \tag{56}$$

where the relation $P_N^{\widehat{+}} = \mathbb{C}P_{N\widehat{+}} + \mathbb{S}P_{N\widehat{-}}$ has been adopted. Correspondingly, we have

$$\Sigma_b^{'} = -i3\left(\frac{g_A}{2f_\pi}\right)^2 \int \frac{d^4k}{(2\pi)^4}\frac{-2(p\cdot k)^2 + k^2(p\cdot k) + 2k^2M^2}{2P_N^{\widehat{+}}M(-p_{N\widehat{+}} - P_{Nb\widehat{+}})D_\pi}. \tag{57}$$

The numerator of the $\Sigma_i^{'}$ (i=a,b) is exactly the same as that of the nucleon self-energy Σ in Eq.(22), while their denominators when added together reproduce the D_N.

Before proceeding, we rescale the $k_{\widehat{-}}$ into $k_{\widehat{-}} = k'_{\widehat{-}}\sqrt{\mathbb{C}}$, and $k_{\widehat{+}}$ into $k_{\widehat{+}} = k'_{\widehat{+}}/\sqrt{\mathbb{C}}$. Integrating over $k'_{\widehat{+}}$, we have

$$\begin{aligned}\Sigma'_a = & -i3\left(\frac{g_A}{2f_\pi}\right)^2 \int \frac{d^2k_\perp dk'_{\widehat{-}}}{(2\pi)^4}\frac{2\pi i}{-2P_N^{'\widehat{+}}M2\omega'_{\widehat{k}}} \\ & \times \frac{-2(\omega'_{\widehat{k}}p^{'\widehat{+}} - p'_{\widehat{-}}k'_{\widehat{-}} - p_\perp k_\perp)^2 + m_\pi^2(\omega'_{\widehat{k}}p^{'\widehat{+}} - p'_{\widehat{-}}k'_{\widehat{-}} - p_\perp k_\perp) + 2m_\pi^2M^2}{p^{'\widehat{+}} - \omega'_{\widehat{k}} - P_N^{'\widehat{+}}} + f_{arc},\end{aligned} \tag{58}$$

and

$$\begin{aligned}\Sigma'_b = & -i3\left(\frac{g_A}{2f_\pi}\right)^2 \int \frac{d^2k_\perp dk'_{\widehat{-}}}{(2\pi)^4}\frac{2\pi i}{-2P_N^{'\widehat{+}}M2\omega'_{\widehat{k}}} \\ & \times \frac{-2(-\omega'_{\widehat{k}}p^{'\widehat{+}} - p'_{\widehat{-}}k'_{\widehat{-}} - p_\perp k_\perp)^2 + m_\pi^2(-\omega'_{\widehat{k}}p^{'\widehat{+}} - p'_{\widehat{-}}k'_{\widehat{-}} - p_\perp k_\perp) + 2m_\pi^2M^2}{-p^{'\widehat{+}} - \omega'_{\widehat{k}} - P_N^{'\widehat{+}}} + f'_{arc}.\end{aligned} \tag{59}$$

where

$$\omega'_{\widehat{k}} = \sqrt{k'^2_{\widehat{-}} + k_\perp^2 + m_\pi^2 - i\epsilon} \tag{60}$$

$$P_N^{'\widehat{+}} = \sqrt{p'^2_{N\widehat{-}} + p_{N\perp}^2 + M^2 - i\epsilon} \tag{61}$$

$$p^{'\widehat{+}} = \sqrt{p'^2_{\widehat{-}} + p_\perp^2 + M^2}. \tag{62}$$

are rescaled variables denoted with primes. Notably all the interpolation parameters ($\mathbb{C}$ and $\mathbb{S}$) are superficially disappeared which results in simplicity in expressions. The f_{arc} or f'_{arc}

are some contributions from the loop integration over the arc at infinity. The functions are independent of pion mass m_π and hence do not contribute to the non-analytic (NA) behaviors. Actually they can be canceled during the process of Pauli-Villars (PV) regularization which will be demonstrated later.

For the remnant part in Eq.(28), we get

$$\Sigma_{RP} = -i3\left(\frac{g_A}{2f_\pi}\right)^2 \int \frac{d^2k_\perp dk'^{\widehat{-}}}{(2\pi)^4} \frac{2\pi i[2(\omega'_{\widehat{k}} p'^{\widehat{+}} - p'^{\widehat{-}}_{\widehat{-}} k'^{\widehat{-}}_{\widehat{-}} - p_\perp k_\perp)\omega'_{\widehat{k}} - p'^{\widehat{+}} m_\pi^2]}{2P'^{\widehat{+}}_N M 2\omega'_{\widehat{k}}} + f''_{arc}. \quad (63)$$

The arc f''_{arc} can also be canceled after the PV regularization being applied.

To get some analytic results, we have to make some assumptions to the variable with frames $p'^{\widehat{-}}_{\widehat{-}}$. One way is to assume

$$\vec{p'} = \left(p'^{\widehat{-}}_{\widehat{-}}, p_\perp\right) = \left(p^{\widehat{-}}_{\widehat{-}}/\sqrt{\mathbb{C}}, p_\perp\right) = \vec{0}. \quad (64)$$

which we may call the "frame X", and it mimics the nucleon rest frame since $p^{\widehat{-}}_{\widehat{-}}/\sqrt{\mathbb{C}} = p^z$ in IFD ($\delta = 0$).

With this assumption, frame X, we are able to solve the splitted off-mass-shell nucleons self-energy analytically. In addition, the Eq.(63) becomes

$$\Sigma_{RP:pole} = -i3(2\pi i)\left(\frac{g_A}{2f_\pi}\right)^2 \int \frac{4\pi \vec{k'}^2 d|\vec{k'}|}{(2\pi)^4} \frac{2\vec{k'}^2 + m_\pi^2}{4\sqrt{\vec{k'}^2 + M^2}\sqrt{\vec{k'}^2 + m_\pi^2}} \quad (65)$$

which does not contribute to the LNA, i.e. $\Sigma^{LNA}_{RP:FrameX} = 0$. The resulting LNA behaviors for each parts in this assumption are summarized in the Tab.2.

The frame X defines a "J" curve

$$\delta = -\arctan\left[\frac{p^z}{\sqrt{p^{z2} + M^2}}\right], \quad (66)$$

which is a semi-infinite line starting from $(\delta,\ p^z) = (0,\ 0)$ and approaching to $(\delta,\ p^z) = (\pi/4,\ -\infty)$. See the black lines in Fig.(7a,7b). The line forming a "J" curve is an isohypse line in the sense that the value on the line remains unchanged with different interpolating angles and the frames. This line is non-trivial as it connects the instant form rest-frame and the LF form. But it also raise questions. Since the LFD is proved to be frame invariance as all the frame variables $p^\pm$ are canceled during calculation, the Σ_a and Σ_b must be invariant on LF including the $(\delta,\ p^z) = (\pi/4,\ -\infty)$ point in frame X. But it is not the case if one compares the Tab. 1 and the second column of Tab.2. It indicates missing contribution from the LF zero mode at $(\delta,\ p^z) = (\pi/4,\ -\infty)$.

In the LFD, we have $p'^{\widehat{-}}_{\widehat{-}} = p^{\widehat{-}}_{\widehat{-}}/\mathbb{C} = p^+/0$. The assumption of frame X requires that $p'^{\widehat{-}}_{\widehat{-}} = 0$, which restricts $p^+ = 0$. This is the so called light-front zero mode. From $p^+ = 0$, we find $\sqrt{(p^z)^2 + M^2} = -p^z$, suggesting that $p^z = -\infty$, which exactly gives the $(\delta,\ p^z) = (\pi/4,\ -\infty)$ as we analyzed. To resolve the issue of the frame dependence on the LFD at $(\delta,\ p^z) = (\pi/4,\ -\infty)$, there must be an additional zero model contribution

$$\Sigma_{Zero\ mode} = -\frac{3g_A^2}{32\pi f_\pi^2}\left(\frac{5}{16\pi}\frac{m_\pi^4 \log[m_\pi^2]}{M}\right) \quad (67)$$

such that

$$\Sigma_a^{LFD} = \Sigma_{Zero\ mode} + \Sigma_a^{(\pi/4,\ -\infty)} \quad (68)$$

LNA $\left(/\frac{-3g_A^2}{32\pi f_\pi^2}\right)$	ID(Frame X) =IFD(rest) =LFD($p^z \to -\infty$)	ID(Frame Y) =IFD($p^z \to \infty$) =LFD($p^z \neq -\infty$)
Σ'_a	$m_\pi^3 + \frac{11}{16\pi}\frac{m_\pi^4 \log[m_\pi^2]}{M}$	$m_\pi^3 + \frac{1}{2\pi}\frac{m_\pi^4 \log[m_\pi^2]}{M}$
Σ'_b	$-\frac{3}{16\pi}\frac{m_\pi^4 \log[m_\pi^2]}{M}$	0
Σ_a	$m_\pi^3 + \frac{11}{16\pi}\frac{m_\pi^4 \log[m_\pi^2]}{M}$	$m_\pi^3 + \frac{3}{8\pi}\frac{m_\pi^4 \log[m_\pi^2]}{M}$
Σ_b	$-\frac{3}{16\pi}\frac{m_\pi^4 \log[m_\pi^2]}{M}$	$\frac{1}{8\pi}\frac{m_\pi^4 \log[m_\pi^2]}{M}$
Σ	$m_\pi^3 + \frac{1}{2\pi}\frac{m_\pi^4 \log[m_\pi^2]}{M}$	$m_\pi^3 + \frac{1}{2\pi}\frac{m_\pi^4 \log[m_\pi^2]}{M}$

Table 2: Anatomy of the nucleon self-energy in LNA terms. The second and third columns show the splitted nucleon self energy in frame X and frame Y. The second and third (forth and fifth) rows show the forward and backward moving on (off) mass shell nucleon self energy. The sixth row is the entire contribution, in agreement with that in Tab. 1.

$$\Sigma_b^{LFD} = -\Sigma_{Zero\ mode} + \Sigma_b^{(\pi/4,\ -\infty)}. \tag{69}$$

Alternatively, we introduce another assumption dubbed the "frame Y" to analyze. Analogous to the frame X, the frame Y is the "interpolating version" of the infinite momentum frame (IMF). Following the definition in [5], the frame Y is

$$k'^{\perp} = \pm(1-y)p'^{\perp},\ dk'^{\perp} = \mp p'^{\perp} dy, \tag{70}$$

with $p'^{\perp} \to \infty$ and $p_\perp = 0$, where the $\pm$ sign are for the forward and backward moving parts respectively. Since $p^{\perp}/\sqrt{\mathbb{C}} = p^z$ in IFD ($\delta = 0$), the frame Y is indeed the usual IMF, i.e. $p^z \to \infty$ in the IFD. The LFD itself has crossover with the frame Y, except for the $p^z = -\infty$ point, which lies out of frame Y but in the frame X. Therefore, the corresponding LNA behavior in frame Y for the on-mass-shell parts are found to be identical with the LFD results. For frame Y, we also summarize the LNA of the Σ'_a and Σ'_b as well as their on-mass-shell counterparts in Tab. 2. Other than LF, the frame Y also covers the infinite momentum frames ($p^z \to \infty$) in the remaining forms including the IFD.

5 Trace the backward and forward moving part numerically

To get numerical results, the divergence in the loop integrations for each part must be coped and better in a covariant way. We begin with Eq.(58), (59), and (63). Considering that these integrations are divergent after the $k_+^{\perp}$ integration, we regularize the remaining divergence by the Pauli-Villars regularization defined in Eq.(33). In real practices, we can just substitute all the m_π^2 with Λ^2 in the integrand of Eq.(58), (59), and (63) (where $k_+^{\perp}$ integrations are done), i.e. to get the integrands for the $1/D_\Lambda$ part. Then subtract them from the original integrand with m_π which corresponds to the $1/D_\pi$ part to get $\Sigma'_{a:1F}$, $\Sigma'_{b:1F}$ and $\Sigma_{RP:1F}$.

After this process, all the arc contributions from the pole integration are removed by the subtraction. However, the remaining integration is still divergent. We follow the Eq.(42) to

raise the power of the PV form factor. With the underlay of this section, we calculate the backward and forward moving nucleon self-energy using Eq.(54). Considering the analytical difficulties in the calculations, we solve them numerically, by varying δ and p_z which represent different forms and frames in the following.

To see the interpolating angle and frame dependence for Σ_a and Σ_b, we need the aid of the interpolating variable ($p'_{\widehat{-}}$) that changes with the form and frame, i.e.,

$$p'_{\widehat{-}} = p_{\widehat{-}}/\sqrt{\mathbb{C}} = \frac{\sqrt{M^2 + p^{z2}}sin\delta + p^z cos\delta}{\sqrt{cos2\delta}}, \tag{71}$$

with p^z the third component of the external momentum $\mathbf{p}$ in the IFD. For the value of masses, $M = 0.94GeV > m_\pi = 0.14$ GeV. The physical quantities are chosen according to [17]: the axial vector charge of the nucleon is $g_A = 1.267$, and the pion decay constant $f_\pi = 0.093$ GeV. We choose the Pauli-Villars parameter to be $\Lambda = 1.03$ GeV, which has also the meaning of the axial mass according to [21]. With those conditions and quantities, we calculate i.e. $\Sigma_{a:4F}$ and $\Sigma_{b:4F}$ numerically.

The results are shown in Fig. 7a and Fig. 7b which are forward and backward decomposition with δ, p^z-profile. The black lines outlining the "J" shape curve correspond to the frame X, while the blue lines correspond to part of the frame Y, which includes the LFD except for $p^z = -\infty$ point as well as the $p^z = \infty$ in other dynamics ($0 \leq \delta < \pi/4$). The later is reaching out of the ranges of the figures and is not pictured. The entire dispersion demonstrate the form and frame dependence of each part of the nucleon self-energy. However, since the Fig. 7a and Fig. 7b are dispersed anti-symmetrically, their summation is flat, independent of the interpolating angle and frame, as shown in Fig. 7c. The value of the flat plane is around -0.232 GeV, which agrees with the analytical result of Σ_{4F}. In the frame Y (IMF in IFD or the LFD), our numerical results suggest that the value for Σ_a and Σ_b are about to be -0.275 GeV and 0.043 GeV respectively, which are in correspondence with the analytical results of Σ_a^{LFD} and Σ_{LFI} respectively. An extrapolation is that the off-mass-shell backward moving part $\Sigma'_b = 0$ in the LFD, totally being suppressed, while the Σ'_a becomes the entire nucleon self-energy.

To investigate the end point behavior which is elusive in previous δ-p_z profile, we use a δ-$p_{\widehat{-}}$ profile instead. This can "amplify" the behavior at the end point of the frame X in LFD (LF zero mode range), as plotted in the Fig. 8a-8b. The frame X become a straight line on a fusiform mountain which shrink into a point (δ function) in the LFD, while the frame Y in the LFD becomes only half of the length as those in previous Fig. 7a-7b. The crossing point of the frame X and Y (black and blue lines) is the zero mode contribution that is hidden in the $-\infty$ of the LFD in previous Fig. 7a-7b.

In addition, we also use the other profile as $p'_{\widehat{-}}$ versus δ, by which we can show the behaviors of the forward and backward moving nucleon self-energy that are independent of the interpolation angle. See Fig. 9a-9b. The sum of them is of course a flat plane as Fig. 7c. To sum up, we list all the numerical results of $\Sigma_{a:4F}$, $\Sigma_{b:4F}$ in frame X and Y in Tab. 3.

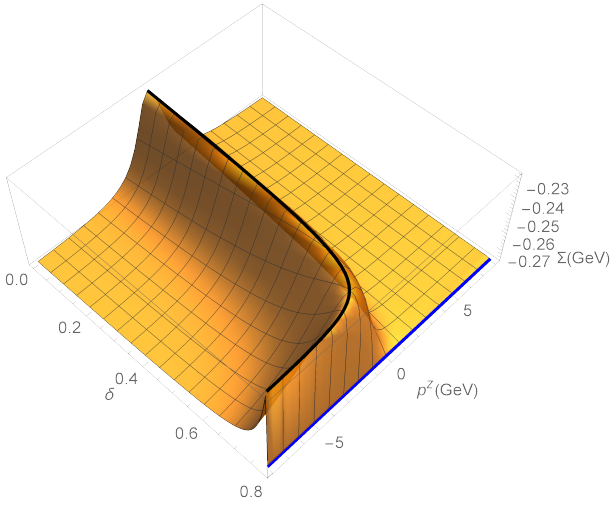

(a)

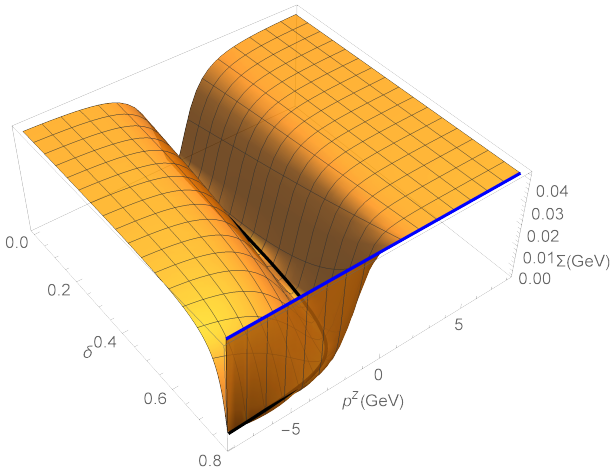

(b)

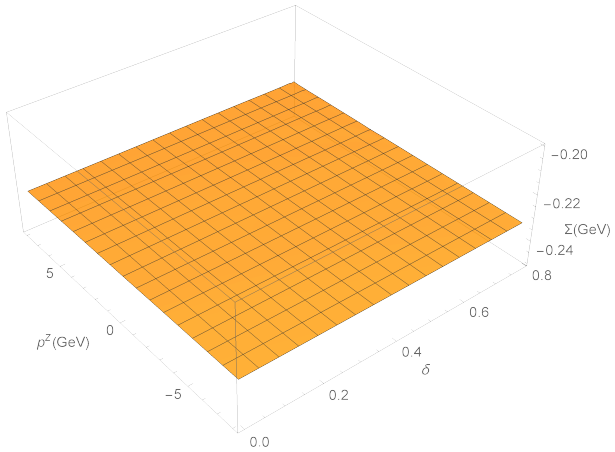

(c)

Figure 7: Numerical calculations (δ versus p^z) for interpolating (a) forward moving part of nucleon self-energy: $\Sigma_{a:4F}$; (b) backward moving part of nucleon self-energy: $\Sigma_{b:4F}$; (c) the entire nucleon self-energy: $\Sigma_{a:4F} + \Sigma_{b:4F}$. Frame X: black lines; frame Y: blue lines.

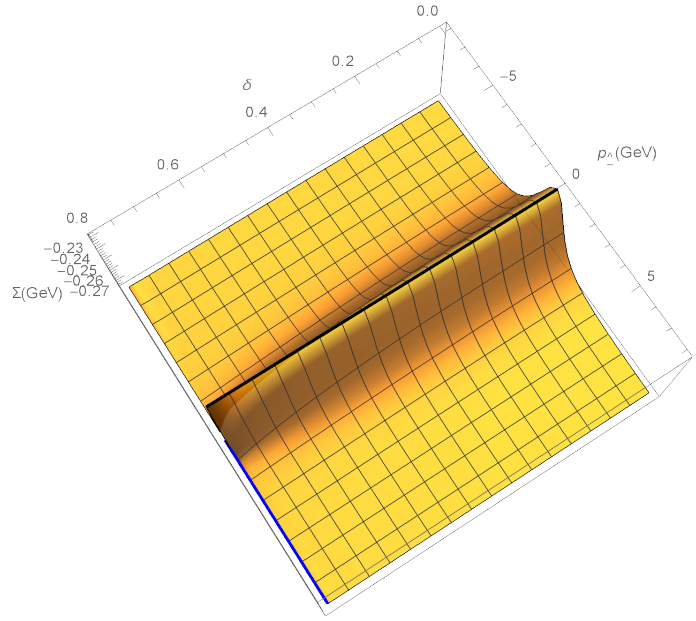

(a)

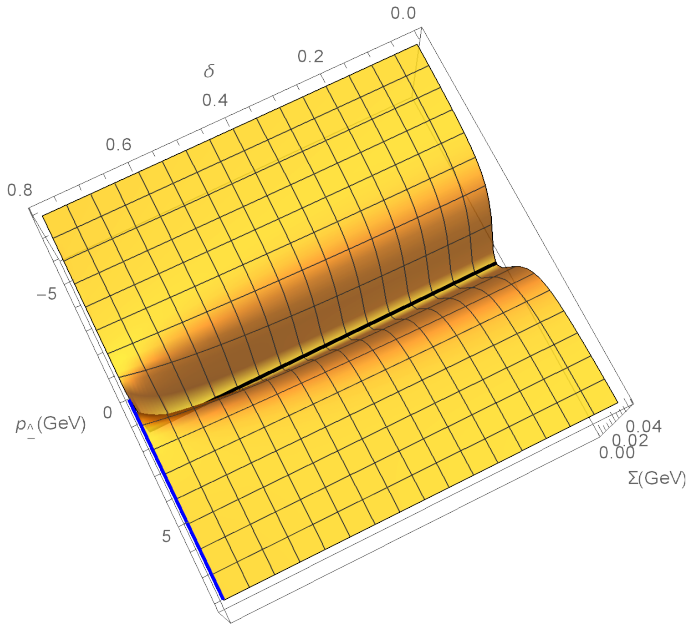

(b)

Figure 8: Numerical calculations (δ versus $p_{\hat{-}}$) for interpolating (a) forward moving part of nucleon self-energy: $\Sigma_{a:4F}$; (b) backward moving part of nucleon self-energy: $\Sigma_{b:4F}$; Frame X: black lines; frame Y: blue lines.

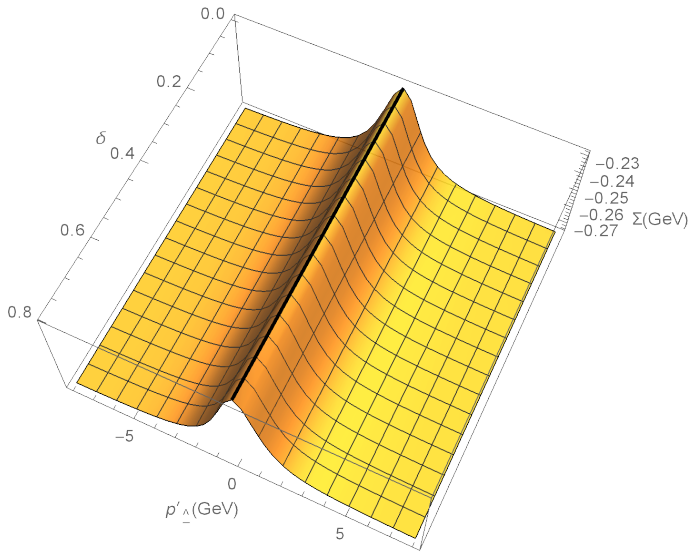

(a)

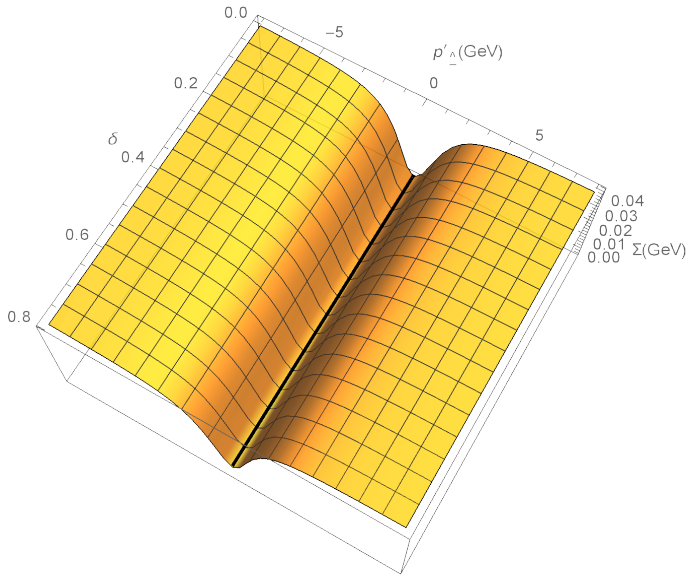

(b)

Figure 9: Numerical calculations (δ versus $p'_{\wedge}$) for interpolating (a) forward moving part of nucleon self-energy: $\Sigma_{a:4F}$; (b) backward moving part of nucleon self-energy: $\Sigma_{b:4F}$; Frame X: black lines; and frame Y is in the infinite $p'_{\wedge}$ which is out of the range.

Numerical results (GeV)	ID(Frame X) =IFD(rest) =LFD($p^z \to -\infty$)	ID(Frame Y) =IFD($p^z \to \infty$) =LFD($p^z \neq -\infty$)
$\Sigma'_{a:4F}$	-0.201	-0.232
$\Sigma'_{b:4F}$	-0.031	0
$\Sigma_{a:4F}$	-0.228	-0.275
$\Sigma_{b:4F}$	-0.004	0.043
Σ_{4F}	-0.232	-0.232

Table 3: Numeric anatomy of the nucleon self-energy. The second and third columns show the splitted nucleon self energy in frame X and frame Y. The second and third (forth and fifth) rows show the forward and backward moving on (off) mass shell nucleon self energy. The sixth row is the entire contribution, in agreement with the flat dispersion as shown in the Fig. 7c.

6 Conclusion

In this paper, we identify the LNA behavior of the LFI loop contribution from the backward nucleon self-energy and the corresponding forward contribution in the LFD. Then with interpolating parametrization, we trace the LNA behaviors for each parts from the LFD to IFD along special lines, which we assume as "frames" X and Y, and identify the emergent LF zero model contribution. With numerical technics, we trace on the entire form-frame profile the each contributions of the nucleon self-energy (in three different manners), which give figurative illustrations about how each part of the nucleon self-energy evolves with respect of forms and frames.

A Anatomy of the reduced nucleon self-energy

A.1 Reducing the nucleon self-energy

We start from the general formulation for the Σ in Eq.(22). Similarly, to regularize the divergence we only need to do the PV regularization twice, or equivalently, multiplying the Pauli-Villars form factor $\left(\frac{-\Lambda^2}{D_\Lambda}\right)^2$ to the Eq.(22), and get

$$\Sigma_{2F} = -i3\Lambda^4 \left(\frac{g_A}{2f_\pi}\right)^2 \int \frac{d^4k}{(2\pi)^4} \frac{-\left[2(p\cdot k)(k\cdot p_N) - (p\cdot p_N)k^2\right] + M^2k^2}{D_N D_\pi D_\Lambda^2}. \tag{72}$$

Noting that

$$k^2 = D_\pi + m_\pi^2 \tag{73}$$

$$p\cdot k = \frac{1}{2}(D_\pi - D_N + m_\pi^2) \tag{74}$$

and omitting the terms that are odd in k, we get

$$\Sigma_{2F} = -\frac{3ig_A^2 M}{32 f_\pi^2 \pi^4}(I'_{2F} + m_\pi^2 I_{2F}). \tag{75}$$

with

$$I_{2F} = \int d^4k \frac{\Lambda^4}{D_N D_\pi D_\Lambda^2} \tag{76}$$

$$I'_{2F} = \int d^4k \frac{\Lambda^4}{D_N D_\Lambda^2}. \tag{77}$$

We apply the interpolating dynamics to calculate the two anatomies of nucleon self-energy.

A.2 Distinguish forward and backward moving nucleon self-energy

We use the time-ordered perturbation theory for our calculations, in specifically the $k'^{\widehat{+}}$ time-ordering. Although it maybe simpler to use Feynman trick to get the analytical result, the time-ordered calculation enable us to trace different directions for the propagating nucleon.

Now we manage the I'_{2F} integration. As an underlay, we first introduce the

$$I'_{1F} = \int d^4k \frac{-\Lambda^2}{D_\Lambda D_N} \tag{78}$$

which can become I'_{2F} by doing a derivative to the integration with respect to Λ^2 as suggested from Eq.(42).

After written with four momentums expanded, we can split the poles with rescaled variables as

$$I'_{1F} = -\Lambda^2 \int d^2k_\perp \int dk'^{\widehat{-}} \int \frac{dk'^{\widehat{+}}}{(k'^{\widehat{+}} - \kappa'^{1+})(k'^{\widehat{+}} - \kappa'^{1-})(k'^{\widehat{+}} - \kappa'^{2+})(k'^{\widehat{+}} - \kappa'^{2-})}, \tag{79}$$

with the form factor poles

$$\kappa'^{2\pm} = \pm\sqrt{k'^2_{\widehat{-}} + k_\perp^2 + \Lambda^2 - i\epsilon} = \pm\omega'_{\widehat{k}\Lambda}. \tag{80}$$

where the κ_+ poles are in the lower half plane (LHP), while the κ_- poles are in the upper half plane (UHP).

To show the time ordering of $k'^{\widehat{+}}$, we first transform the integrand into

$$I'_{1F} = -\Lambda^2 \int d^2k_\perp \int dk'^{\widehat{-}}_{-} \int dk'^{\widehat{+}} \left(\frac{1}{k'^{\widehat{+}} - \kappa'^{1+}} - \frac{1}{k'^{\widehat{+}} - \kappa'^{1-}}\right) \frac{1}{\kappa'^{1+} - \kappa'^{1-}} \times \left(\frac{1}{k'^{\widehat{+}} - \kappa'^{2+}} - \frac{1}{k'^{\widehat{+}} - \kappa'^{2-}}\right) \frac{1}{\kappa'^{2+} - \kappa'^{2-}}. \tag{81}$$

As only the multiplication of the terms containing poles from the different sides of the real axis will contribute, the integration with total factor can be simplified as

$$-\frac{3ig_A^2 M}{32f_\pi^2\pi^4} I'_{1F} = -\frac{3ig_A^2 M(-\Lambda^2)}{32f_\pi^2\pi^4} \int d^2k_\perp \int dk'^{\widehat{-}}_{-} \int dk'^{\widehat{+}} - \frac{1}{\kappa'^{1+} - \kappa'^{1-}} \frac{1}{\kappa'^{2+} - \kappa'^{2+}} \times \left[\frac{1}{(k'^{\widehat{+}} - \kappa'^{1-})(k'^{\widehat{+}} - \kappa'^{2+})} + \frac{1}{(k'^{\widehat{+}} - \kappa'^{1+})(k'^{\widehat{+}} - \kappa'^{2-})}\right] \tag{82}$$

$$= \Sigma_{1F}^{N\Lambda:-+} + \Sigma_{1F}^{N\Lambda:+-} \tag{83}$$

where the superscript "$N\Lambda : -+$" means that the nucleon pole (N) and the form factor pole (F) are chosen as κ'^{1-} $(-)$ and κ'^{2+} $(+)$, and vice versa. Using the residue theorem to integrate the $k_{\widehat{+}}$, catching the nucleon poles, we get

$$\Sigma_{1F}^{N\Lambda:-+} + \Sigma_{1F}^{N\Lambda:+-} = -\frac{3ig_A^2 M(-\Lambda^2)}{32f_\pi^2\pi^4} \int d^2k_\perp \int dk'^{\widehat{-}}_{-} \frac{-2\pi i}{2\omega'_{\widehat{k}\Lambda} 2P'^{\widehat{+}}} \left(\frac{1}{p'^{\widehat{+}} - \omega'_{\widehat{k}\Lambda} - P'^{\widehat{+}}} + \frac{-1}{p'^{\widehat{+}} + \omega'_{\widehat{k}\Lambda} + P'^{\widehat{+}}}\right). \tag{84}$$

which appears to have no $\mathbb{S}$ and $\mathbb{C}$ in the integrand, and corresponds to the forward moving positive-energy diagram ($\Sigma_{1F}^{N\Lambda:-+}$) and the backward moving "Z" graph ($\Sigma_{1F}^{N\Lambda:+-}$), the same with previous Fig. 5a and Fig. 5b respectively.

Similarly we define

$$I_{1F} = \int d^4k \frac{-\Lambda^2}{D_N D_\pi D_\Lambda}. \tag{85}$$

Using the PV subtraction defined in Eq.(33),

$$I_{1F} = -\Lambda^2 \int d^4k \frac{1}{D_\Lambda - D_\pi} \left(\frac{1}{D_N D_\pi} - \frac{1}{D_N D_\Lambda}\right) \tag{86}$$

where in the bracket the first term is very similar as, while the second term is the same as the previous I'_{1F}. Therefore, we can easily get

$$-\frac{3ig_A^2 M}{32f_\pi^2\pi^4} m_\pi^2 I_{1F} = \frac{m_\pi^2}{D_\Lambda - D_\pi} \left(\Sigma_{1F}^{N\pi:-+} + \Sigma_{1F}^{N\pi:+-} - \Sigma_{1F}^{N\Lambda:-+} - \Sigma_{1F}^{N\Lambda:+-}\right). \tag{87}$$

where the $\Sigma_{1F}^{N\pi:-+}$ and $\Sigma_{1F}^{N\pi:+-}$ are obtained by substituting all the $\omega'_{\widehat{k}\Lambda}$s in $\Sigma_{1F}^{N\Lambda:-+}$ and $\Sigma_{1F}^{N\Lambda:+-}$ with $\omega'_{\widehat{k}}$, and the $\Sigma_{1F}^{N(\pi-\Lambda):\mp\pm} = \frac{m_\pi^2}{m_\pi^2 - \Lambda^2} \left(\Sigma_{1F}^{N\pi:\mp\pm} - \Sigma_{1F}^{N\Lambda:\mp\pm}\right)$.

To sum up, we have

$$\Sigma_{1F} = \Sigma_{1F}^{N\Lambda:-+} + \Sigma_{1F}^{N\Lambda:+-} + \frac{m_\pi^2}{D_\Lambda - D_\pi} \left(\Sigma_{1F}^{N\pi:-+} + \Sigma_{1F}^{N\pi:+-} - \Sigma_{1F}^{N\Lambda:-+} - \Sigma_{1F}^{N\Lambda:+-}\right). \tag{88}$$

LNA $\left(/\frac{-3g_A^2}{32\pi f_\pi^2}\right)$	ID(Frame X) =IFD(rest) =LFD($p^z \to -\infty$)	ID(Frame Y) =IFD($p^z \to \infty$) =LFD(p^z independent)
$\Sigma_{2F}^{N\Lambda:\mp\pm}$	0	0
$\Sigma_{2F}^{N(\pi-\Lambda):-+}$	$m_\pi^3 + \frac{3}{4\pi}\frac{m_\pi^4 \log[m_\pi^2]}{M}$	$m_\pi^3 + \frac{1}{2\pi}\frac{m_\pi^4 \log[m_\pi^2]}{M}$
$\Sigma_{2F}^{N(\pi-\Lambda):+-}$	$-\frac{1}{4\pi}\frac{m_\pi^4 \log[m_\pi^2]}{M}$	0
Σ_{2F}	$m_\pi^3 + \frac{1}{2\pi}\frac{m_\pi^4 \log[m_\pi^2]}{M}$	$m_\pi^3 + \frac{1}{2\pi}\frac{m_\pi^4 \log[m_\pi^2]}{M}$

Table 4: Summary of the LNA terms of the $\Sigma_{2F}^{N\Lambda:\mp\pm}$, $\Sigma_{2F}^{N(\pi-\Lambda):\mp\pm}$ and their summation in frame X and Y. The second and third columns show that the forward and backward nucleon moving parts in frame X and frame Y (that both connect the IFD and the LFD) do not contribute to the LNA. The forth and fifth columns show the LNAs for the forward and backward nucleon-pion propagating part in frame X and frame Y. The summations of the LNA terms are listed in the sixth column, where the results in two frames are the same. To get the LF zero mode contribution, similarly, one can use the relations: $\Sigma_{Zero\ mode}^{N\Lambda} = \pm\Sigma_{2F:frameX}^{N\Lambda:+-}$, and $\Sigma_{Zero\ mode}^{N(\pi-\Lambda)} = \pm\Sigma_{2F:frameX}^{N(\pi-\Lambda):+-}$. Therefore the LNA for the LF zero mode contributions are 0 and $\mp\frac{1}{4\pi}\frac{m_\pi^4 \log[m_\pi^2]}{M}$ (in unit of $\frac{3g_A^2}{32\pi f_\pi^2}$) to the $\Sigma_{2F}^{N\Lambda:\mp\pm}$ and the $\Sigma_{2F}^{N(\pi-\Lambda):\mp\pm}$ at the $p^z \to -\infty$ of the frame X.

where the first and last two terms correspond to I'_{1F} and I_{1F} respectively.

Since the Σ_{1F} is still divergent, we similarly do the derivatives to raise the power of D_Λ using Eq.(42). Practically we change the order of the integration and the derivation, i.e. we do the derivative to the integrand of the four terms in Eq.(88) and then perform the perpendicular integration to get

$$\Sigma_{2F} = \Sigma_{2F}^{N\Lambda:-+} + \Sigma_{2F}^{N\Lambda:+-} + \frac{m_\pi^2}{D_\Lambda - D_\pi}\left(\Sigma_{2F}^{N\pi:-+} + \Sigma_{2F}^{N\pi:+-} - \Sigma_{2F}^{N\Lambda:-+} - \Sigma_{2F}^{N\Lambda:+-}\right). \quad (89)$$

A.3 Summary of LNA and numerical results for the anatomies of the reduced nucleon self-energy

We choose frame X and Y as follows to obtain the corresponding non-analytic behaviors for each time-ordered diagrams. Following the previous section, we apply the frame X to calculate the four terms in Eq.(89). Their LNA behaviors for each parts are summarized in the second row of Tab. 4.

Similarly, we apply the frame Y to the forward and backward parts of the Σ_{2F}. Their LNA behaviors for each parts are summarized in the third row of Tab. 4. The We find that all the terms corresponding to "Z" graphs, i.e. $\Sigma_{2F}^{N\Lambda:+-}$ and $\Sigma_{2F}^{N(\pi-\Lambda):+-}$, are suppressed, in agreement with our numerical results in Tab. 5. Our results agree with those in paper[17].

We also adopt the physics quantities/variables the same as the previous section to calculate the 4 anatomies of Σ_{2F} as $\Sigma_{2F}^{N\Lambda:\mp\pm}$ and $\Sigma_{2F}^{N(\pi-\Lambda):\mp\pm}$ in the form-momentum δ, p^z profile, which correspond to the nucleon propagating part $1/D_N$ and nucleon-pion propagating part $1/(D_N D_\pi)$ respectively. The curvature for the $\Sigma_{2F}^{N\Lambda:-+}$ and $\Sigma_{2F}^{N(\pi-\Lambda):+-}$ are the same with

Numerical results (GeV)	ID(Frame X) =IFD(rest) =LFD($p^z \to -\infty$)	ID(Frame Y) =IFD($p^z \to \infty$) =LFD(p^z independent)
$\Sigma_{2F}^{N\Lambda:-+}$	-0.763	-1.105
$\Sigma_{2F}^{N\Lambda:+-}$	-0.342	0
$\Sigma_{2F}^{N(\pi-\Lambda):-+}$	0.026	0.031
$\Sigma_{2F}^{N(\pi-\Lambda):+-}$	0.005	0
Σ_{2F}	-1.074	-1.074

Table 5: Summary of numerical results of $\Sigma_{2F}^{NF:\mp\pm}$, $\Sigma_{2F}^{N(\pi-\Lambda):\mp\pm}$ and their summation in frame X and Y. The second and third columns show the numerical results of forward and backward nucleon moving parts in frame X and frame Y (that both connect the IFD and the LFD). The forth and fifth columns show the forward and backward nucleon-pion propagating part in frame X and frame Y. The summations of the four terms in both frames are listed in the sixth column, where both results are the same, indicating that the entire nucleon self-energy is invariant under different frames and forms, corresponding to the Fig. 7c. Besides, the summations of the second and third as well as the forth and the fifth columns in two frames are also the same. The LF zero mode contributions at $p^z = -\infty$ to the $\Sigma_{2F}^{NF:\mp\pm}$ and $\Sigma_{2F}^{N(\pi-\Lambda):\mp\pm}$ are ∓ 0.342 GeV and ± 0.005 GeV respectively.

that in Fig. 7a, which has a convex "J" curve that protruding upwards. On the other hand, for the $\Sigma_{2F}^{N\Lambda:+-}$ and $\Sigma_{2F}^{N(\pi-\Lambda):-+}$, they correspond to the concave "J" curve in Fig. 7b that is protruding downwards. Since for each "J", no matter which direction they are protruding, we only care about two values, i.e. the values on the black line that defining the frame X and the blue line for frame Y. Therefore, we summarize the two values for the four anatomies of the Σ_{2F} in the following Tab. 5. Adding the four parts, i.e. $\Sigma_{2F}^{N\Lambda:\mp\pm}$ and $\Sigma_{2F}^{N(\pi-\Lambda):\mp\pm}$ together, we get the plane, similar as the Fig. 7c, except that the value of the plane is changed to around -1.074GeV, which when doing the derivatives using Eq.(42) agrees with our analytical result in Eq.(52).

To sum up, we find that the total interpolating nucleon self-energy is independent of the δ and p^z, while individual time ordered contributions depend on the interpolating angle and the frame.

References

[1] Dirac, Paul AM. "Forms of relativistic dynamics." Reviews of Modern Physics 21.3 (1949): 392.

[2] Melde, T., et al. "Electromagnetic nucleon form factors in instant and point form." Physical Review D 76.7 (2007): 074020.

[3] Ji, Chueng-Ryong, and Chad Mitchell. "PoincarsŠ invariant algebra from instant to light-front quantization." Physical Review D 64.8 (2001): 085013.

[4] Ji, Xiangdong. "Parton physics on a Euclidean lattice." Physical review letters 110.26 (2013): 262002.

[5] Drell, Sidney D., Donald J. Levy, and Tung-Mow Yan. "Theory of deep-inelastic lepton-nucleon scattering and lepton pair annihilation processes. II. Deep-inelastic electron scattering." Physical Review D 1.4 (1970): 1035.

[6] Rossi, G. C., and M. Testa. "Note on lattice regularization and equal-time correlators for parton distribution functions." Physical Review D 96.1 (2017): 014507.

[7] Carlson, Carl E., and Michael Freid. "Lattice corrections to the quark quasidistribution at one loop." Physical Review D 95.9 (2017): 094504.

[8] Thomas, Anthony W. "Chiral symmetry and the bag model: A new starting point for nuclear physics." Advances in nuclear physics. Springer, Boston, MA, 1984. 1-137.

[9] Schreiber, Andreas W., and Anthony W. Thomas. "Spin dependent structure functions in the cloudy bag model." Physics Letters B 215.1 (1988): 141-144.

[10] Myhrer, F., and A. W. Thomas. "A possible resolution of the proton spin problem." Physics Letters B 663.4 (2008): 302-305.

[11] Hornbostel, Kent. "Nontrivial vacua from equal time to the light cone." Physical Review D 45.10 (1992): 3781.

[12] Ji, Chueng-Ryong, and Alfredo Takashi Suzuki. "Interpolating scattering amplitudes between the instant form and the front form of relativistic dynamics." Physical Review D 87.6 (2013): 065015.

[13] Ji, Chueng-Ryong, Ziyue Li, and Alfredo Takashi Suzuki. "Electromagnetic gauge field interpolation between the instant form and the front form of the Hamiltonian dynamics." Physical Review D 91.6 (2015): 065020.

[14] Li, Ziyue, Murat An, and Chueng-Ryong Ji. "Interpolating helicity spinors between the instant form and the light-front form." Physical Review D 92.10 (2015): 105014.

[15] Ji, Chueng-Ryong, et al. "Interpolating quantum electrodynamics between instant and front forms." Physical Review D 98.3 (2018): 036017.

[16] C.-R.Ji, "Pedestrian Approach to Particle Physics", published by Asia Pacific Center for Theoretical Physics, ISBN 978-89-958822-0-7 93420, 249 pages, 2007.

[17] Ji, Chueng-Ryong, W. Melnitchouk, and A. W. Thomas. "Equivalence of pion loops in equal-time and light-front dynamics." Physical Review D 80.5 (2009): 054018.

[18] Ji, Chueng-Ryong, Wally Melnitchouk, and Anthony W. Thomas. "Anatomy of relativistic pion loop corrections to the electromagnetic nucleon coupling." Physical Review D 88.7 (2013): 076005.

[19] Ji, Chueng-Ryong, et al. "Pauli-Villars regularization elucidated in Bopp-Podolsky¡¯s generalized electrodynamics." The European Physical Journal C 79.10 (2019): 871.

[20] F.Bopp, Ann.Phys.**430**(5), 345(1940);B.Podolsky, Phys. Rev. **62**,68(1942).

[21] Alberg, Mary, and Gerald A. Miller. "Taming the pion cloud of the nucleon." Physical review letters 108.17 (2012): 172001.

[22] Alexandrou, Constantia, and Christos Kallidonis. "Low-lying baryon masses using N f= 2 twisted mass clover-improved fermions directly at the physical pion mass." Physical Review D 96.3 (2017): 034511.

[23] Zee, Anthony. Quantum field theory in a nutshell. Vol. 7. Princeton university press, 2010: 212.